

Shear bands in magnesium alloy AZ31^①

YANG Ping(杨平)¹, MAO Weimin(毛卫民)¹,
REN Xueping(任学平)¹, TANG Quanbe(唐全波)²

(1. School of Materials Science and Engineering, University of Science and Technology Beijing,
Beijing 100083, China;

2. The 56th Institute of Chongqing, Chongqing 400039, China)

Abstract: During deformation of magnesium at low temperatures, cracks always develop at shear bands. The origin of the shear bands is the $\{10\bar{1}1\}$ twinning in basal-oriented grains and the mobility of this type of twin boundary is rather low. The most frequent deformation mechanisms in magnesium at low temperature are basal slip and $\{10\bar{1}2\}$ twinning, all leading to the basal texture and therefore the formation of shear bands with subsequent fracture. The investigation on the influences of initial textures and grain sizes reveals that a strong prismatic initial texture of $\langle0001\rangle$ parallels to TD and fine grains of less than 5 μm can restrict the formation and expansion of shear bands effectively and therefore improve the mechanical properties and formability of magnesium.

Key words: magnesium alloy; deformation; texture; microstructure

CLC number: TG 111.7; TG 146.2

Document code: A

1 INTRODUCTION

Magnesium often shows unsatisfactory plasticity due to its hexagonal structure with less independent slip systems and the frequently observed $\{10\bar{1}2\}$ twinning provides merely a relative shear strain of 0.129. It is well known that below the temperature of dynamic recrystallization the dominant deformation mechanisms in polycrystalline magnesium are basal slip and $\{10\bar{1}2\}$ twinning^[1]. Thus the magnesium subjected to these types of deformation mechanisms is studied mostly. However, fracture in magnesium is not directly related with the deformation inhomogeneities produced by these deformation mechanisms, rather it links with shear band formation^[2-5]. So far the information about the origin of shear bands and the $\{10\bar{1}1\}$ twinning is rather limited, particularly on the orientations within the shear bands. It was reported that during deformation at about 240 °C the (sub) grains within the shear bands were disoriented for about 35° with respect to their matrix^[6]. It was determined by means of trace analysis in single crystals of magnesium that the $\{10\bar{1}1\}$ twinning would proceed when compressed along c -axis and subsequently $\{10\bar{1}2\}$ twinning and basal slip would occur in twined regions^[2, 3]. Fracture may form from them at ambient temperature. Kelley et al^[2] called it $\{10\bar{1}$

1} banding. Due to the direct relation between shear bands and fractures, it is crucial to explore the nature of shear bands and the method of preventing their formation. This work aims to investigate the features of shear band formation and their dependence on initial textures and grain sizes. The orientational characteristics of shear bands are discussed and the way of preventing their formation is proposed.

2 EXPERIMENTAL

The tested material is a magnesium alloy AZ31. The initial materials are a hot rolled plate of 12 mm in thickness and hot extruded bars of d 20 mm and d 33 mm respectively. The initial average grain sizes are 25, 5 and 34 μm after an anneal on the hot rolled plate and the d 33 mm extruded bar. Basal texture of $\langle0001\rangle$ parallel to rolling plane existed in hot rolled plate and fiber textures of $\langle1\bar{1}00\rangle/\langle11\bar{2}0\rangle$ parallel to extrusion axis were present in extruded bars. The extruded d 20 mm bar contained 13% large elongated deformed grains. Samples of dimension of 15 mm × 10 mm × 6 mm were sectioned in different ways, called TR and NR from hot rolled plate and having textures of $\langle0001\rangle/\text{TD}$ in TR and $\langle0001\rangle/\text{ND}$ in NR. Samples XZ1 and ZY1 were prepared from d 20 mm bar and samples XZ and ZY were machined from d 33 mm bar. The initial textures in samples TR,

① **Foundation item:** Project(50171009) supported by the National Natural Science Foundation of China; project(2002AA305501) supported by the Hi-tech Research and Development Program of China

Received date: 2004-02-01; **Accepted date:** 2004-05-18

Correspondence: YANG Ping, Professor; Tel: +86-10-62332705; E-mail: yangp@mater.ustb.edu.cn

XZ, XZ1 were similar, and the initial textures in samples ZY and ZY1 were also akin with $\langle 0001 \rangle$ being parallel to ND, for details referring to Ref. [7]. Channel die compression was applied on these samples to realize a plane-strain compression. MoS_2 paste was used to reduce the friction between the samples and die form. Deformation was conducted at 97 °C and 185 °C under strain rate of 0.01 s^{-1} . Six incomplete pole figures of $(10\bar{1}0)$, (0002) , $(1\bar{1}01)$, $(11\bar{2}0)$, $(1\bar{1}02)$, $(1\bar{1}03)$ were measured by X-ray diffraction and were used to calculate orientation distribution function (ODF). Section $\Phi_2 = 0^\circ$ of ODF was exploited to represent orientation distribution. Samples were prepared using AC-2 electrolyte and picric acetic solution and observed by optic and electron scanning microscope on lateral section of samples. Orientation mapping by EBSD technique was applied to reveal local orientation and orientation relationships.

3 RESULTS AND DISCUSSION

3.1 Morphological features of shear bands and their dependence on initial textures

Fig. 1 shows the microstructures of deformed samples TR and NR at two temperatures. It is seen that the shear bands are more in sample NR than that in sample TR. At 97 °C the shear bands were straight and sometimes cross-sectioned. As indicated in Ref.

[7] that the initial prismatic texture of $\langle 0001 \rangle \parallel \text{TD}$ in sample TR was stable during double prismatic slip and disfavored the formation of shear band. However, due to a slight allowance of TD extension, certain amount of $\{10\bar{1}2\}$ twinning proceeded gave rise to basal orientation and subsequent formation of shear bands. Nevertheless, the shear bands are less in sample TR. Shear bands form invariantly in the basal oriented grains. As sample NR is basal oriented initially, massive shear bands form directly. In another sample XY with initial texture of $\{0001\}$ is parallel to TD, which is particularly suitable for basal slip, large amounts of shear bands are also developed. At 185 °C straight shear bands are able to expand apparently as shown in Fig. 1 (d), whereas undeveloped shear bands are located mainly at grain boundaries in sample TR.

Fig. 2 exhibits the $\sigma - \varepsilon$ curves of samples TR and NR. At 97 °C sample NR was broken at strain of about 14% and fracture was along 45° with respect to RD because the straight $\{10\bar{1}1\}$ twin boundaries can not expand to carry plastic deformation. The sample TR, in contrast, deformed relatively uniform. At 185 °C distinct softening happened in sample NR which was correlated with the expansion of shear bands as observed in Fig. 1 (d). Through the expansion of shear bands large amount of plastic deformation was achieved in the

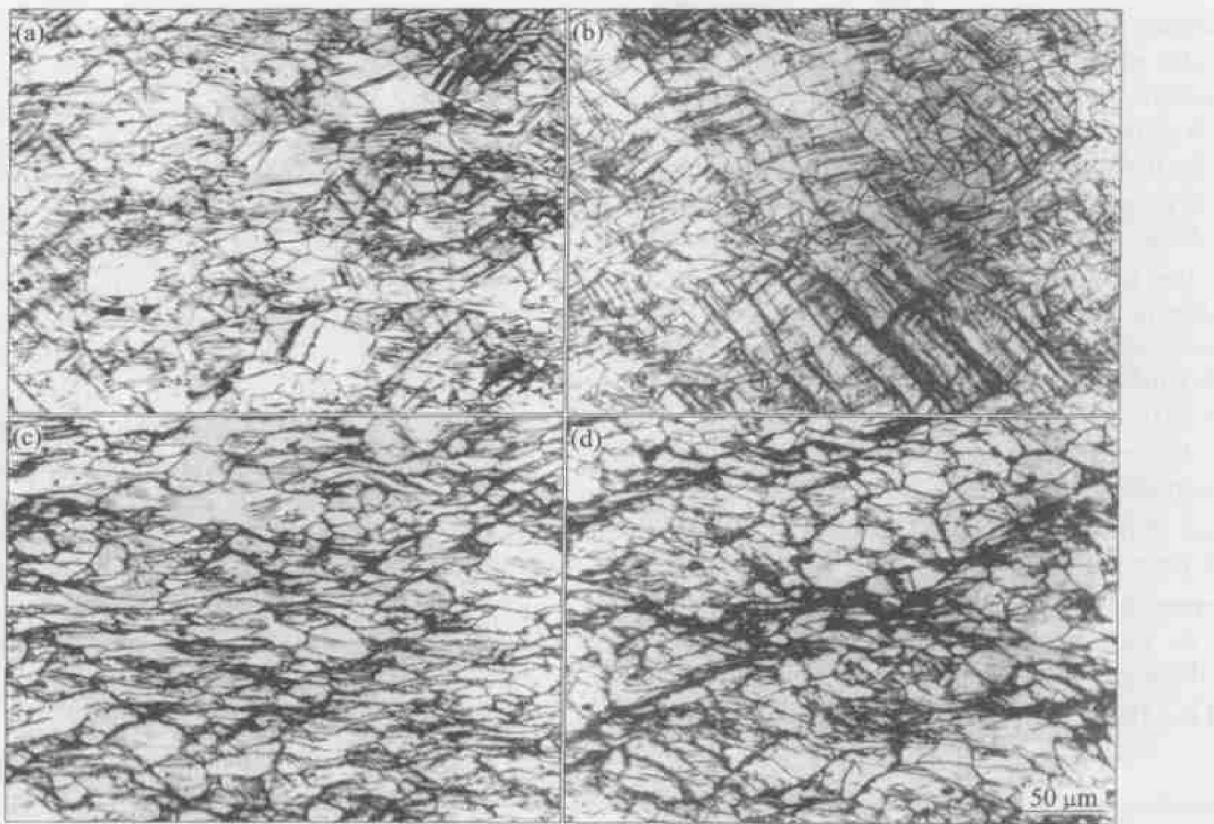


Fig. 1 Microstructures of deformed samples TR and NR at different temperatures
(a) —TR, 97 °C, 0.25; (b) —NR, 97 °C, 0.25; (c) —TR, 185 °C, 0.60; (d) —NR, 185 °C, 0.60

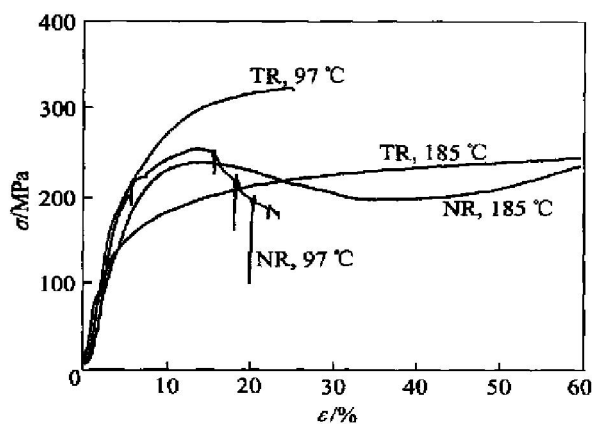


Fig. 2 σ — ϵ curves in samples TR and NR

region of shear bands. Strictly speaking, the decline of stress at 185 °C in sample NR did not correspond to the dynamic recrystallization, but only to a localized deformation, because the subgrains at this temperature are not able to grow (Fig. 3(a)). Fig. 3(b) illustrates a crack formed at shear bands at the strain of 0.80 in sample ZY. The crack has an angle of about 45° with respect to RD.

3.2 Influence of grain size on shear band formation

As the shear bands are localized, deformed zones like other deformation inhomogeneities are easily formed in large grains. The density and size of shear bands were declined in the order of samples ZY



Fig. 3 Microstructures of shear bands at 185 °C and different strain
 (a) —Sample NR, 0.60;
 (b) —Crack in sample ZY, 0.80

(mean grain size 34 μm), NR (25 μm) and ZY1 (5 μm) respectively, indicating obviously a relationship of density with grain size. Fig. 4 shows the microstructures in deformed fine-grained samples XZ1 and ZY1. It is seen that $\{10\bar{1}1\}$ twins or shear bands are very few in fine-grained regions. In contrast, they can be easily formed in large elongated grains (the lower part of Fig. 4(a)) which accounts to 13% (volume fraction) in d_{20} mm bar. At 185 °C no shear bands expanded significantly indicating that fine grains of less than about 5 μm can prevent the formation and expansion of shear bands effectively.

By comparing the textures in coarse- and fine-grained samples (see Fig. 5), it is clear that the

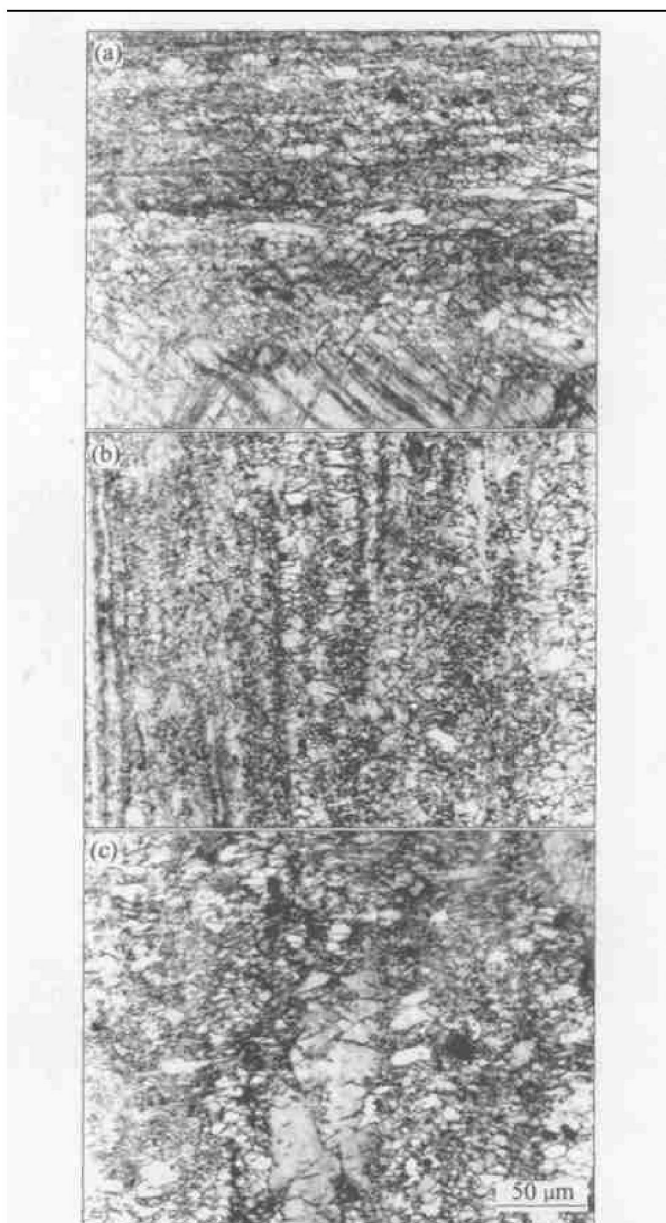


Fig. 4 Microstructures in fine-grained samples at different temperatures and strain
 (a) —XZ1, 97 °C, 0.25; (b) —ZY1, 97 °C, 0.25;
 (c) —ZY1, 185 °C, 0.60

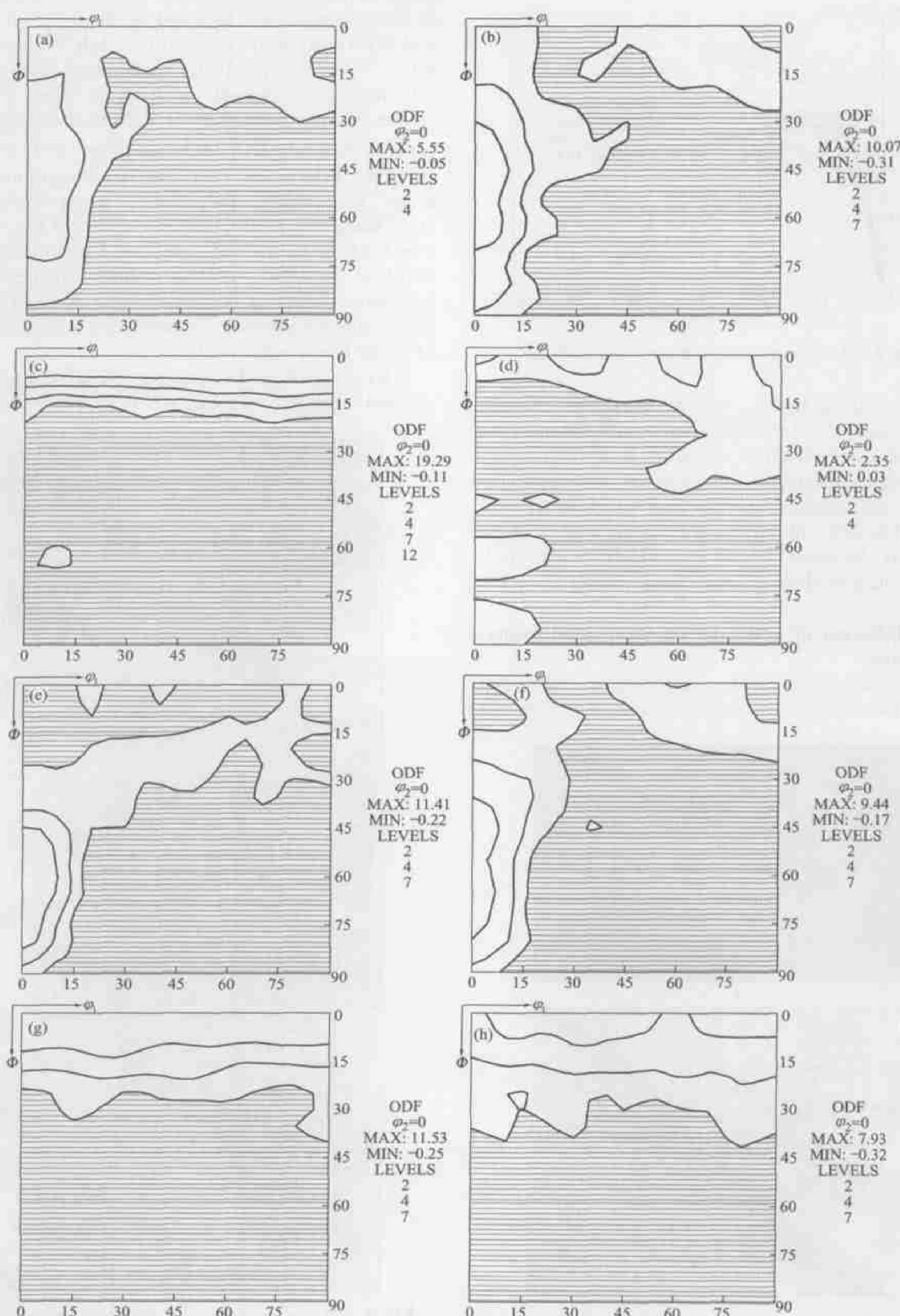


Fig. 5 Grain orientation distributions in deformed samples with different initial textures

(a)—XZ1, 97 °C, $\epsilon=0.25$; (b)—XZ1, 185 °C, $\epsilon=0.60$; (c)—ZY1, 97 °C, $\epsilon=0.25$; (d)—ZY1, 185 °C, $\epsilon=0.60$; (e)—XZ, 97 °C, $\epsilon=0.25$; (f)—XZ, 185 °C, $\epsilon=0.60$; (g)—ZY, 97 °C, $\epsilon=0.25$; (h)—ZY, 185 °C, $\epsilon=0.60$

prevention of shear band formation and expansion by grain refinement is independent of initial texture, although the latter exerts strong influence on the shear band formation.

Fig. 6 shows the σ — ε curves of coarse and fine grained samples ZY, ZY1 for comparison. At 97 °C the least plastic sample ZY1 was broken at strain of 0.22 instead of 0.13% in the case of sample ZY. If the detrimental effect of 13% elongated large grains in sample ZY1 can be excluded, the plasticity should be further improved. The shorter softening range of strain and a low stress decrease in sample ZY1 at 185 °C are evidently due to the less expanded shear bands, i. e. the grain refinement.

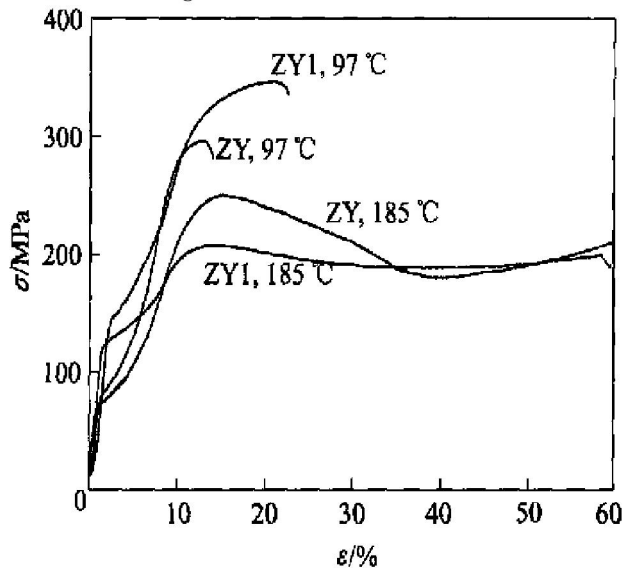


Fig. 6 σ — ε curves of samples ZY1 and ZY

3.3 Shear bands and $\{10\bar{1}1\}$ twinning

In Refs. [4, 5], the nomenclature 'shear band' is often used instead of $\{10\bar{1}1\}$ twinning^[3]. However they are correlated. The $\{10\bar{1}1\}$ twinning is the origin of the shear bands. At room temperature shear bands can not fully develop and the fracture often initiates directly from $\{10\bar{1}1\}$ twins. In Ref. [7] the $\{10\bar{1}1\}$ twinning was already determined by trace analysis in accordance with previous results on single crystals^[2, 3]. Fig. 7(a) gives another example showing that the cross-sectioned shear bands should be related with $\{10\bar{1}1\}$ twinning by trace analysis in the basal oriented grain (Fig. 5(a)). It also reveals that prismatic oriented grains (light color) twined at first producing basal oriented grain (dark color). Then $\{10\bar{1}1\}$ twins formed in the dark-colored grains with basal orientation. Fig. 7(b) indicates that the shear bands at their early stage are thin bands. Therefore, they should have nothing to do with any type of slips. As temperature increases twins can expand to form shear bands. Although attention begins to be paid to the interaction between basal dislocation and the

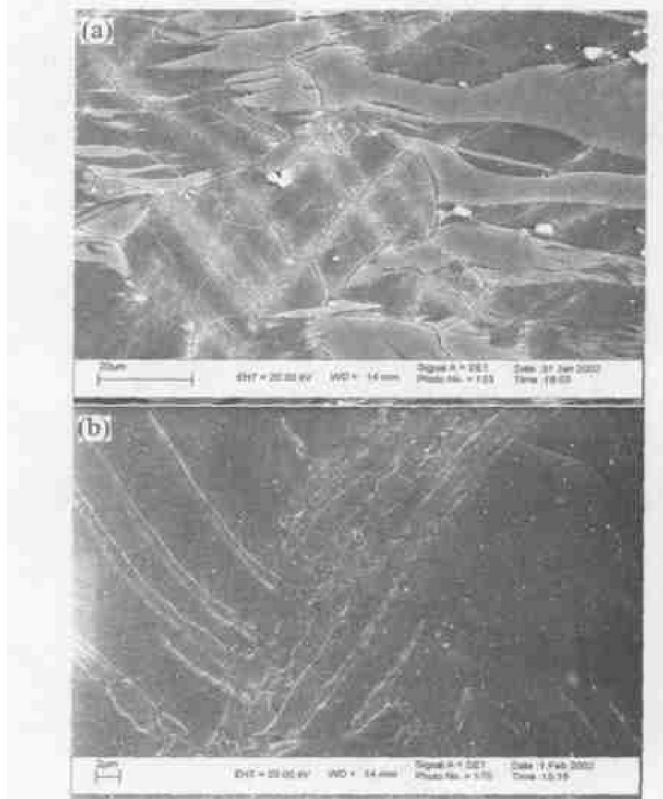


Fig. 7 Relationship of shear bands with $\{10\bar{1}1\}$ twins at strain of 0.25
(a) —TR, 97 °C; (b) —ZY, 185 °C

$\{10\bar{1}2\}/\{10\bar{1}1\}$ twin boundaries^[8-11] including computer simulation, it is still not clear why the $\{10\bar{1}1\}$ twin boundaries can not move easily, whilst those of $\{10\bar{1}2\}$ quickly spread all over the whole grains in magnesium. The expansion of shear bands at high temperature was schematically described in Ref. [6].

3.4 Orientations in shear bands

As analyzed above the origin of shear bands is the $\{10\bar{1}1\}$ twinning whose orientations can be easily computed as shown in Fig. 8(a). These twin orientations are linked with their basal-oriented host by a 56.1° $\langle 11\bar{2}0 \rangle$ relationship. Fig. 8(b) demonstrates the deformation texture in sample NR showing weak textures of 60° apart from ND. Because of the difficulty of twin boundary movement the volume fraction of twins is rather low and therefore their influence on texture is hard to detect. In addition, as the twin width is only about 1 μm , EBSD technique combined with normal tungsten gun in SEM fails to measure single orientation. Finally, under the condition of compression twin orientations (Fig. 8(a)) are unstable and are easily changed by other deformation mechanisms such as $\{10\bar{1}2\}$ twinning and/or basal slip^[2, 3]. At a higher temperature when shear bands can expand the orientations within shear bands can be changed clearly. So, orientations related with shear bands change from time to time.

Fig. 9 shows an orientation mapping on sample ZY1 within a large elongated grain with basal orientation. Most regions at shear bands did not give orientation solutions (called blind spots or zero solution)

due to high density of crystallographic defects. If extrapolation was applied to discard zero solutions some new orientations within the shear bands can be shown clearly as shown in Fig. 9(c).

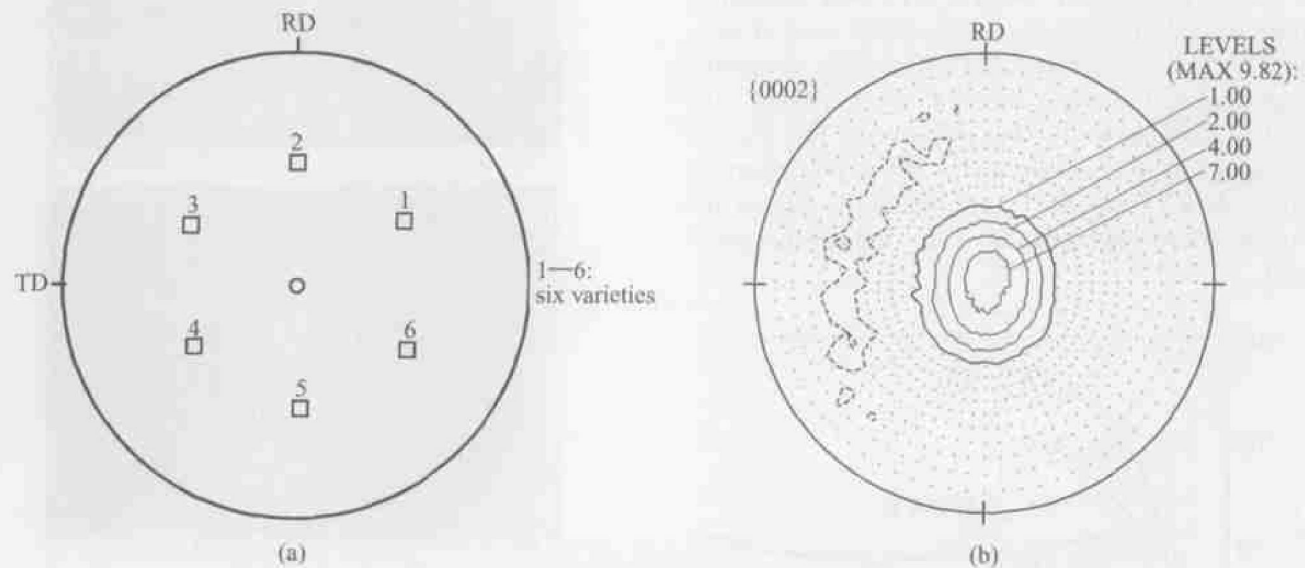


Fig. 8 New orientations by $\{10\bar{1}1\}$ twinning from initially basal oriented grain
(a) Calculated result, twin variants;
(b) Measured result, sample NR, 97 °C, $\epsilon=0.25$

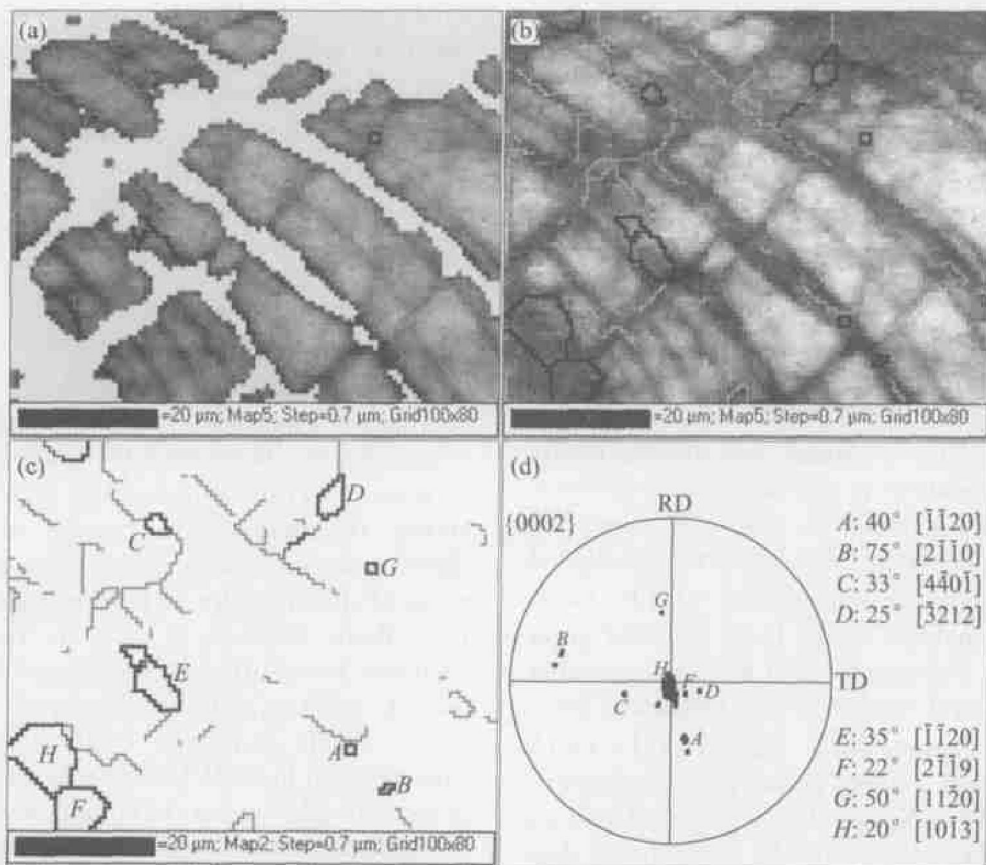


Fig. 9 Orientation mapping of sample ZY1 at 97 °C and strain of 0.25
(a) Kikuchi band contrast, grey color; position of zero solution; (b) Zero solutions discarded by extrapolation;
(c) Distribution of grain boundaries; (d) (0002) pole figure and orientation relationships

Note that the extrapolation can only lead to incorrect grain sizes and not incorrect orientations. Fig. 9(d) shows the orientations in the shear bands. From the calculated orientation relationships listed in Fig. 9(d) it is seen that only orientations A , B , E , G own nearly the twinning rotation axis of $[11\bar{2}0]$, but not the 56.1° for $\{10\bar{1}1\}$ twinning. This may be explained by further rotation around $\langle11\bar{2}0\rangle$.

From the results given above it is known that the fracture in deformed magnesium always forms along the shear bands. The shear bands are related with $\{10\bar{1}1\}$ twinning which occurs in the basal-oriented grains. At elevated temperature plastic deformation is achieved within the expanded shear bands in samples with basal texture. Since deformation mechanisms in polycrystalline magnesium are mainly basal slip and $\{10\bar{1}2\}$ twinning, which all lead to basal texture, the best way to prevent the formation of shear bands is to produce an initial sample with strong prismatic texture of $\langle0001\rangle/\text{TD}$ and a fine grain size of less than $5 \mu\text{m}$. In this way the properties and formability can be improved apparently. It is frequently reported that grain refinement in magnesium improves the strength and formability significantly^[12-14]. The latter is attributed to the low temperature superplasticity^[15, 16]. However, it was also found that the mechanical behaviors of fine-grained samples processed differently with equal average grain sizes were totally different^[9, 10]. They realized that texture played an important role in this case. No explanation is given to the difference in shear band formation.

4 CONCLUSIONS

1) The $\{10\bar{1}1\}$ twins in basal oriented grains are the origins of both shear bands and the fractures formed in deformed magnesium at low temperatures. The most frequently observed deformation mechanisms in magnesium, namely the basal slip and the $\{10\bar{1}2\}$ twinning, all give rise to basal texture and therefore lead to intrinsic insufficient plasticity of magnesium. The difficulty in the movement of $\{10\bar{1}1\}$ twin boundaries is responsible for the poor plasticity of magnesium.

2) An initial material with strong prismatic texture of $\langle0001\rangle/\text{TD}$ and a fine grain size of less than about $5 \mu\text{m}$ can restrict the formation and expansion of shear bands and thus improve the mechanical properties and formability of magnesium.

Acknowledgment

Part work was performed in IMM RWTH Aachen, Germany.

REFERENCES

- [1] Stalmann A, Sebastian W, Friedrich H, et al. Properties and processing of magnesium wrought products for automotive applications[J]. *Adv Eng Mater*, 2001, 3(12): 969-974.
- [2] Kelley E W, Hosford W F Jr. Plane strain compression of magnesium and magnesium alloy crystals[J]. *Trans AIME*, 1968, 242(1): 5-13.
- [3] Wonsiewicz B C, Backofen W A. Plasticity of magnesium crystals[J]. *Trans AIME*, 1967, 239(9): 1422-1431.
- [4] Gehrmann R, Gottstein G. Texture and microstructure development during plastic deformation of magnesium [A]. *Proceedings of 12th Inter Conf on Textures of Materials* [C]. Montreal, Canada: NRC Research Press, 1999. 665-670.
- [5] Klimanek P, Poetzsch A. Microstructure evolution under compressive plastic deformation of magnesium at different temperatures and strain rates[J]. *Mater Sci and Eng*, 2002, A324(1): 145-150.
- [6] Ion S E, Humphreys F J, White S H. Dynamic recrystallisation and the development of microstructure during the high temperature deformation of magnesium[J]. *Acta Metall*, 1982, 30(10): 1909-1919.
- [7] Yang P, Cui F E, Bian J H, et al. Relationships between deformation mechanisms and initial textures in polycrystalline magnesium alloys AZ31[J]. *Trans Nonferrous Met Soc China*, 2003, 13(2): 280-284.
- [8] Serra A, Bacon D J. Computer simulation of screw dislocations with twin boundaries in HCP metals[J]. *Acta Metal Mater*, 1995, 43(12): 4465-4481.
- [9] Pond R C, Celotto S. Interfacial deformation mechanisms in hexagonal close packed metals [J]. *Metall Mater Trans*, 2002, 33A(3): 801-807.
- [10] Serra A, Bacon D J, Pond R C. Twins as barriers to basal slip in hexagonal close packed metals[J]. *Metall Mater Trans*, 2002, 33A(3): 809-812.
- [11] Yoo M H, Morris J R, Ho K M, et al. Nonbasal deformation modes of HCP metals and alloys: role of dislocation source and mobility [J]. *Metall Mater Trans*, 2002, 33A(3): 813-822.
- [12] Kubota K, Mabuchi M, Higashi K. Processing and mechanical properties of fine-grained magnesium alloys[J]. *J Mater Sci*, 1999, 34(10): 2255-2262.
- [13] Mukai T, Yamanoi M, Watanabe H, et al. Ductility enhancement in AZ31 magnesium alloy by controlling its grain structure[J]. *Scripta Mater*, 2001, 45(1): 89-94.
- [14] Chino Y, Mabuchi M. Influences of grain size on mechanical properties of extruded AZ91 alloy after different extrusion processes[J]. *Advanced Engineering Materials*, 2001, 3(12): 981-983.
- [15] Koike J, Kobayashi T, Mukai T, et al. The activity of nonbasal slip systems and dynamic recovery at room temperature in fine-grained AZ31B magnesium alloys [J]. *Acta Mater*, 2003, 51(4): 2055-2065.
- [16] Mabuchi M, Ameyyama K, Iwasaki H, et al. Low temperature superplasticity of AZ91 magnesium alloy with non-equilibrium grain boundaries[J]. *Acta Mater*, 1999, 47(7): 2047-2057.

(Edited by LONG Huai-zhong)